

## Deuterium retention in the divertor tiles of JET ITER-Like wall



A. Lahtinen<sup>a,\*</sup>, J. Likonen<sup>b</sup>, S. Koivuranta<sup>b</sup>, A. Hakola<sup>b</sup>, K. Heinola<sup>a</sup>, C.F. Ayres<sup>c</sup>,  
A. Baron-Wiechec<sup>c</sup>, J.P. Coad<sup>c</sup>, A. Widdowson<sup>c</sup>, J. Räisänen<sup>a</sup>, JET Contributors<sup>d,1</sup>

<sup>a</sup> Department of Physics, University of Helsinki, P.O. Box 43, 00014 University of Helsinki, Finland

<sup>b</sup> VTT Technical Research Centre of Finland Ltd., P.O. Box 1000, 02044 VTT, Finland

<sup>c</sup> CCFE, Culham Science Centre, Abingdon, OX14 3DB, UK

<sup>d</sup> EUROfusion Consortium, JET, Culham Science Centre, Abingdon, OX14 3DB, UK

### ARTICLE INFO

#### Article history:

Received 15 July 2016

Revised 31 March 2017

Accepted 16 April 2017

Available online 16 May 2017

#### Keywords:

JET

Fuel retention

Erosion

Deposition

### ABSTRACT

Divertor tiles removed after the second JET ITER-Like Wall campaign 2013–2014 (ILW-2) were studied using Secondary Ion Mass Spectrometry (SIMS). Measurements show that the thickest beryllium (Be) dominated deposition layers are located at the upper part of the inner divertor and are up to  $\sim 40\ \mu\text{m}$  thick at the lower part of Tile 0 exposed in 2011–2014. The highest deuterium (D) amounts ( $> 8 \cdot 10^{18}\ \text{at./cm}^2$ ), in contrast, were found on the upper part of Tile 1 (2013–2014), where the Be deposits are  $\sim 10\ \mu\text{m}$  thick. D was mainly retained in the near-surface layer of the Be deposits but also deeper in tungsten (W) and molybdenum (Mo) layers of the marker coated tiles, especially at W–Mo layer interfaces. D retention for the ILW-2 divertor tiles is higher than for the first campaign 2011–2012 (ILW-1) and probable reasons for the difference are that SIMS measurements for the ILW-2 samples were done deeper than for the ILW-1 samples, some of the tiles were exposed during both ILW-1 and ILW-2 and therefore had a longer exposure time, and the differences between ILW-1 and ILW-2 campaigns e.g. in strike point distributions and injected powers.

© 2017 The Authors. Published by Elsevier Ltd.

This is an open access article under the CC BY-NC-ND license.

(<http://creativecommons.org/licenses/by-nc-nd/4.0/>)

### 1. Introduction

Retention of the plasma fuel in the plasma facing components (PFC) has a key role affecting economical and safe operation of a fusion reactor. Due to the radioactivity of tritium (T), its accumulation has to be restricted below a pre-determined safety limit, e.g., total in vessel limit of 1 kg in ITER. When the T amount in the vessel structures is too high, they need to be cleaned and that will cause breaks to the operation.

Fuel retention in an ITER-like environment has been studied at JET since 2011 in connection with the JET ITER-Like Wall (ILW) project [1] where the same metallic first wall material mix as in ITER is used: tungsten (W) in the divertor and beryllium (Be) in the main chamber components. The first JET–ILW operational period in 2011–2012 (ILW-1) was followed by a shutdown in 2012 during which a poloidal selection of first wall and divertor tiles were removed for post-mortem analyses. In the global gas balance

experiments during the campaign and post-mortem analyses after the campaign, the fuel retention was observed to be reduced by a factor of 10–20 compared to the previous JET operation with the all-carbon wall (JET–C) [2–4]. The highest deposition of Be and the largest amounts of retained fuel were found on Tiles 0 and 1 in the upper inner divertor [3,4].

In the next JET–ILW campaign in 2013–2014 (ILW-2), the injected power to the plasma discharges was higher and strike point positions different, which might have altered material migration, the composition of the deposited layers and the amount of retained fuel. In the 2014 shutdown, a number of tiles were removed for post-mortem analyses to study these effects. This work focuses on the retention profile of deuterium (D) on the divertor tiles removed during the 2014 shutdown.

### 2. Experimental methods

The deuterium concentrations were determined from the selected JET–ILW divertor tiles removed during the 2014 shutdown. The analyzed tiles and the so-called S-coordinate system are shown in the poloidal cross section of the divertor in Fig. 1. Tiles 0, 3, 7 and 8 were exposed during both ILW-1 and ILW-2 campaigns

\* Corresponding author.

E-mail address: [aki.lahtinen@helsinki.fi](mailto:aki.lahtinen@helsinki.fi) (A. Lahtinen).

<sup>1</sup> See appendix of F. Romanelli et al., 25th IAEA Fusion Energy Conference, 2014, Russia

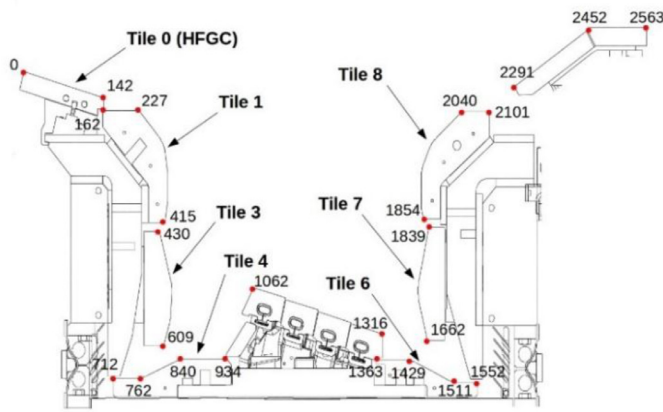


Fig. 1. The JET-ILW divertor tile configuration and the S-coordinate system.

while Tiles 1, 4 and 6 were exposed only during the ILW-2 period. Deposits on Tiles 0, 3, 7 and 8 were not removed between the campaigns and the tiles contained D from the ILW-1 campaign. The ILW-2 (ILW-1) campaign comprised of 19.4 (19) hours of plasma time from which 14.2 (13) hours were in the divertor phase and 5.2 (6) hours in the limiter phase. Strike point distributions for the ILW-1 and ILW-2 campaigns are shown in Fig. 2. During the ILW-2 (ILW-1) the inner strike point was on Tiles 3 and 4 (Tile 3) and the outer strike point predominantly on Tile 6 (Tile 5). The ILW-1 campaign contained a limited number of high current pulses with plasma currents up to 3.5 MA, magnetic field up to 3.2 T and Neutral Beam Injection (NBI) heating up to 26 MW combined with Ion Cyclotron Resonance Heating (ICRH) up to 3.5 MW [5]. The ILW-2 contained larger number of high power pulses with plasma currents up to 4 MA, magnetic field up to 3.7 T, and NBI heating power up to 27 MW, ICRH up to 7 MW and Lower Hybrid Current Drive (LHCD) heating power up to 3 MW [6]. At the end of the ILW-2 campaign, there was a hydrogen plasma campaign that comprised of about 300 plasma discharges.

Tiles 1, 3, 4, 6, 7 and 8 had special marker coatings on top of a carbon fibre composite (CFC) substrate for erosion/deposition studies. Tiles 1, 3, 6, 7 and 8 had a CFC (bulk)/Mo (3  $\mu\text{m}$ )/W (12  $\mu\text{m}$ )/Mo (4  $\mu\text{m}$ )/W (4  $\mu\text{m}$ ) layer structure and Tile 4 had molybdenum as the plasma-facing material with a CFC (bulk)/Mo (3  $\mu\text{m}$ )/W (12  $\mu\text{m}$ )/Mo (4  $\mu\text{m}$ ) layer structure. Tile 0 was a regular tile with a CFC (bulk)/Mo (3  $\mu\text{m}$ )/W (10–15  $\mu\text{m}$ ) structure.

Cylindrical samples with a diameter of 17 mm were cut from the tiles using a hollow drill. The deuterium concentrations of the samples were studied with Secondary Ion Mass Spectrometry (SIMS) using a double focusing magnetic sector instrument VG Ionex IX-70S at VTT Technical Research Centre of Finland (VTT). A 5 keV  $\text{O}_2^+$  primary beam was used and the intensities of the positive secondary ions at mass-to-charge ratios of 1 (H), 2 (D), 9 (Be), 12 (C), 58 (Ni), 98 (Mo) and 183 (W) were measured as a function of time. The current of the primary beam was 500 nA and the beam was raster-scanned over an area of  $300 \times 400 \mu\text{m}^2$ . A 10% electronic gate was used to avoid crater wall effects. After the SIMS measurements, the depths of the craters were measured with a profilometer.

D-implanted Be, Mo and W samples, which were analyzed with Heavy Ion Elastic Recoil Detection Analysis (HI-ERDA), were used for quantification of the SIMS measurements. Implanted samples were used to determine relative sensitivity factors (RSF) for D in Be, W and Mo. These RSFs were then used to determine D concentrations in the Be, W and Mo layers of the ILW samples. In the layer interfaces, where materials are mixed, weighted average was used. Uncertainties are estimated to be about 10%, assum-

ing that the measurement settings are nearly constant during the measurements. The uncertainties in the quantification of the SIMS measurements are related to matrix effects arising from impurities and mixing of the materials, which might affect the secondary ion yields compared to the D-implanted Be, Mo and W samples.

### 3. Results and discussion

#### 3.1. Inner divertor

A SIMS depth profile from the lower part of Tile 0 (S-coordinate 135 mm) is shown in Fig. 3a. The depth profile shows a  $\sim 40 \mu\text{m}$  thick Be dominated deposition layer on top of the W coating. A layer of codeposited H and Be is seen at the surface due to the H phase at the end of the ILW-2 and the main D peak is located near the surface at about a depth of  $2 \mu\text{m}$ . After the main peak, the intensity of the D signal remains constant throughout the deposition layer and there is no significant change in its intensity within the W, Mo and C layers. Nickel originating from the Inconel-steel components of the vessel is also present in the layers. The CFC/Mo/W layer structure of Tile 0 can be seen at the SIMS depth profile: after the Be deposition layer there is  $\sim 10 \mu\text{m}$  thick W layer and thin Mo interlayer before the CFC substrate. SIMS depth profiles do not show sharp interfaces between the layers due to the surface roughness, pores and imperfections of the CFC substrate, crater wall effects in SIMS measurements and probable mixing of the layers. This is best observed from the slow decay of the Be, W and Mo signals when proceeding deeper into the substrate. Penetration of Be through W/Mo structure up to a depth of  $100 \mu\text{m}$  and extension of the original W(10–15  $\mu\text{m}$ )/Mo(3  $\mu\text{m}$ ) layer structure to tens of microns due to the surface roughness and porosity have also been observed after the ILW-1 with glow discharge optical emission spectrometry (GDOES) analyses [7].

The thickness of the Be deposition layer is the largest in the lower part of Tile 0 and in the upper part of Tile 1. Tile 1 was exposed only during 2013–2014 and the thickest measured Be deposits there are about  $10 \mu\text{m}$ . The thickness of the deposit decreases to  $\sim 2 \mu\text{m}$  at the lower part of Tile 1. In addition to the regions with strong deposition, both Tiles 0 and 1 have areas where Be deposition is very low and the thickness of the deposition layer is almost zero. The intensity of the near-surface D peak is higher in the lower part of Tile 1 but after the peak the intensity decreases faster than in the upper part of the tile. In Tile 0, the intensity of the near-surface D peak is about the same in all the measurement points but in the regions with thick deposits the intensity stays at a high level deep inside the material, whereas in the low deposition regions the intensity decreases faster after the peak. In thick deposits of Tile 0, the D peak occurs at around  $1.5\text{--}2 \mu\text{m}$  and there are deposits containing H at the surface. Whereas in the low deposition areas, the depth of the D peak is  $\sim 0.2 \mu\text{m}$  and the depletion of D at the surface is probably partly due to the isotopic exchange effects. In Tile 1, the depth of the D peak is about  $0.5 \mu\text{m}$  in the upper part of the tile and decreases to  $0.2 \mu\text{m}$  in the lower part of the tile. This indicates that there have been more Be deposition on Tile 0 ( $1.5\text{--}2 \mu\text{m}$ ) than Tile 1 ( $0.2\text{--}0.5 \mu\text{m}$ ) during the H phase at the end of ILW-2.

Fig. 3b shows a SIMS depth profile from the center of Tile 3 (S=524 mm). The Be deposition layer on top of W is  $\sim 1 \mu\text{m}$  thick and the intensity of the Be signal decreases slowly, indicating rough surface and mixing of Be with W. Due to the H campaign, the H peak is again seen at the surface while the D peak now emerges at  $\sim 0.4 \mu\text{m}$ . The intensity of the D signal decreases slowly after the peak but the behavior of the D intensity in the deeper material can not be deduced because of the short, under  $10 \mu\text{m}$ , measurement depth. The intensities of C and Ni show peaks at the surface and after that intensities decrease slowly to a back-

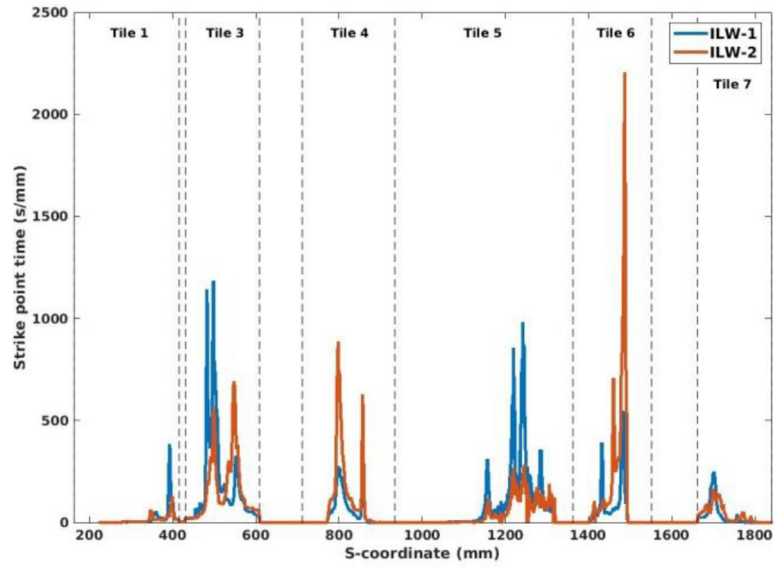


Fig. 2. The strike point distribution for ILW-1 and ILW-2 campaigns.

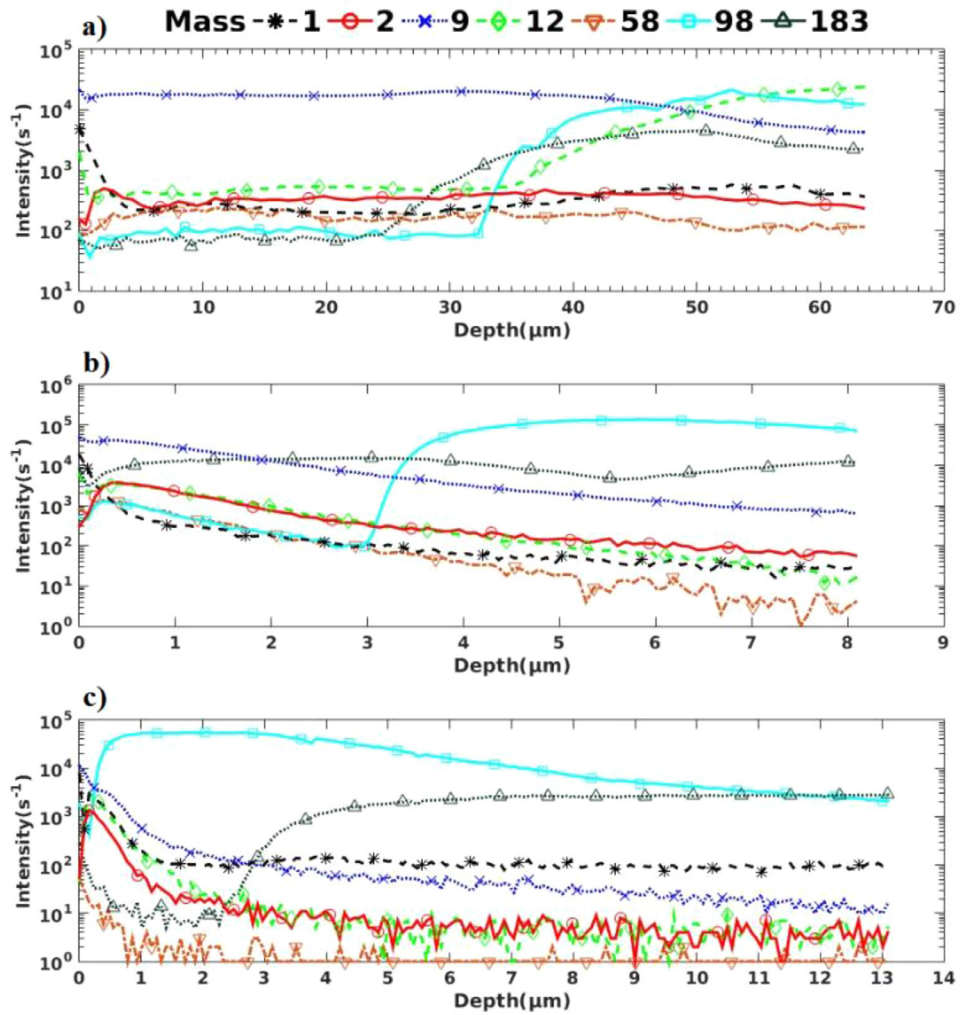


Fig. 3. SIMS depth profiles from a) Tile 0 (exposed in 2011–2014) (S-coordinate 136 mm), b) Tile 3 (2011–2014) (S = 524 mm) and c) Tile 4 (2013–2014) (S = 737 mm).

ground level. The W/Mo/W layer structure of the tile can be seen from the depth profiles.

On Tile 3, the thickness of the Be deposition layer is the highest, about 3  $\mu\text{m}$ , in the upper part of the tile and decreases to about 1  $\mu\text{m}$  at the lower part of the tile. The intensity of the near-surface D peak is about the same in all measurement points from Tile 3. Similar to Tile 1, the depth of the D peak in samples from Tile 3 is 0.2–0.5  $\mu\text{m}$ . Measurements from the topmost part of Tile 3 show erosion of the plasma-facing W layer with Be deposits covering the surface. For a measurement point from the S-coordinate 445 mm, the original 4  $\mu\text{m}$  thick W layer is almost completely eroded. Optical microscopy from cross-sectional samples prepared for the upper part of Tile 3 also indicates only small remnants of the topmost W layer, the Mo layer has also partly been eroded in some areas, and that there is Be co-deposited layer on top of the topmost W layer as observed in the SIMS measurements [8]. Studied Tile 3 was exposed during both ILW-1 and ILW-2 and it is difficult to say when the W layer was eroded but GDOES analysis after the ILW-1 showed erosion of Tile 3 with Mo-coating [7]. It is notable that the strike point time in the eroded area on the topmost part of Tile 3 has been low during both ILW-1 and ILW-2 (see Fig. 2).

Fig. 3c shows a SIMS depth profile from the shadowed part of Tile 4 ( $S = 737$  mm) in the corner of the inner divertor floor. Here, the Be deposition layer is less than 1  $\mu\text{m}$  thick. The intensity of the Be signal at the surface is lower and decreases faster than in Fig. 3a and 3b. Low deposition in the inner divertor corner observed after both ILW-1 and ILW-2 campaigns is different from the observations made after operations with the carbon-wall when deposits in this region were thick [9]. This is attributed to the lower main chamber source and the reduced chemical erosion of Be compared to C [10]. Similarly to Tiles 0, 1 and 3, the H peak is seen at the surface but now also the main D peak is visible very close to the surface. In addition to the surface H peak, the intensity of the H signal exhibits another peak around the same depth as the main D peak. The intensity of the D signal decreases fast to the very small background level after the peak. H signal at depths deeper than  $\sim 2$   $\mu\text{m}$  in Fig. 3c is almost one order of magnitude higher than D signal. This deep H background in Fig. 3c and in other analyzed samples is mainly due to H background level in the SIMS analysis chamber. Deposited C and Ni are also seen at the surface. The intensity of Ni is very low and the intensities of Ni and C decrease faster to a background level than in Tiles 0, 1 and 3. Tile 4 has Mo as plasma-facing coating and deposited W is seen at the surface.

Overall, deposition of Be, C and Ni on Tile 4 is low – the thickness of the Be deposition layer is negligibly small in most of the measurement points on Tile 4. In the inner end of the tile, there are some Be deposits but the thickness of the layer is less than 1  $\mu\text{m}$ . Change of the strike point from Tile 3 (ILW-1) to Tile 4 (ILW-2) has not affected significantly the Be deposition and the highest Be deposition occurs still at the upper inner divertor. The depletion of D at the surface in Tile 4 is lower than in Tiles 0, 1 and 3, and the D peak is very close to the surface at the depth of less than 0.2  $\mu\text{m}$ . There are significant differences in the intensity of the main D peak in different measurement points on Tile 4. The intensity is low at the strike point area and higher at the both sides of the strike point and in the shadowed part of the tile. On the other hand, in the inner strike point area and in the shadowed part of the tile, the intensity decreases quickly to the background level. The SIMS depth profiles from the outer end of the tile show also small peaks in intensity of D signal at the Mo–W interface.

### 3.2. Outer divertor

Fig. 4a shows a SIMS depth profile measured close to the main outer strike point at the center part of Tile 6 ( $S = 1475$  mm) in the outer divertor floor. Be is seen at the surface mixed with W. The

intensity of the Be signal at the surface is about the same as in Fig. 3a and 3b, and it decreases slowly. W/Mo/W layer structure of the sample can also be seen in the figure. The thickness of the plasma-facing W layer is  $\sim 3.5$   $\mu\text{m}$ , so  $\sim 0.5$   $\mu\text{m}$  of the original W layer has been eroded at this point. Similarly to the inner divertor tiles, H peak can be seen on the surface and the D peak near the surface but here the difference between the surface value and the peak value of the D intensity is small. The intensity of the D peak is lower than in the SIMS depth profiles from the inner divertor tiles in Fig. 3 and the intensity decreases quickly to the background level. Low D retention in the strike point areas on divertor floor Tiles 4 and 6 is probably due to high surface temperature as it has been shown that concentration of implanted D decreases when irradiation temperature is increased [11]. The intensities of C and Ni are like in Fig. 3b from Tile 3 at the surface but decrease slowly when moved deep down.

For most of the samples from Tile 6, the thickness of the Be deposits was less than 1  $\mu\text{m}$  and the intensity of the W signal increased sharply close to the surface. The intensity of the Be signal decreased slowly, indicating rough surface and mixing of the Be with W/Mo structure. The thickest measured Be deposits were over 10  $\mu\text{m}$  thick at  $S = 1516$  mm which is 29 mm outward from the predominant outer strike point location at the  $S = 1487$  mm. With respect to ILW-1, the Be deposition on Tile 6 during the ILW-2 was found to be higher and this is due to the increased outer strike point time on the tile. In the outer strike point area at the central part of the tile, the intensity of the near-surface peak of D is low and intensity decreases quickly to the background level. In the other parts of Tile 6, the intensity of the D peak is higher and the intensity decreases slowly. The depth of the D peak is less than 0.2  $\mu\text{m}$  except in the measurements from the thick Be deposits where the depth is  $\sim 0.4$   $\mu\text{m}$ .

Fig. 4b shows a SIMS depth profile from near the center of Tile 7 ( $S = 1765.5$  mm). The depth profile resembles the one from Tile 3 in Fig. 3b, but the Be layer on top of W is thinner. The H peak is seen again at the surface and the D peak near to the surface. Similarly to Fig. 4a, the difference between the surface value and the peak value of the D intensity is small. The intensity decreases slowly and stays clearly on a higher level than in Fig. 4a. The intensities of the C and Ni are similar to Fig. 3b.

Fig. 4c shows a SIMS depth profile from the lower part of Tile 8 ( $S$ -coordinate 1877 mm). Be is seen at the surface and its intensity decreases rapidly. Similarly to Fig. 4a and 4b, the D peak is very close to the surface and the difference of the peak value and the surface value of the intensity is small. In addition to the near-surface peak, other D peaks are seen at the W–Mo and Mo–W interfaces. The intensities of the C and Ni are similar to those in Fig. 4a and 4b at the surface but decrease faster in Fig. 4c.

The strong surface H peak is about similar in all the samples and after the surface peak intensity decreases quickly and then stays at about a constant level. Most of this hydrogen background is due to the hydrogen in the SIMS analysis chamber but some part of it might be due to the in-deep migrated H from the H plasma experiments. It is likely that besides the H experiments at the end of ILW-2 also air exposure after the removing of the tiles from the vessel has contributed to the surface H peak. The effect of air exposure is probably not very high because the surfaces had already high hydrogen and low deuterium concentration from the plasma experiments. In the case of high surface D concentration, air exposure could cause exchange of some part of the surface D with H from the air.

In the outer divertor Tiles 7 and 8, the thickness of the Be deposits is less than 1  $\mu\text{m}$  and the D peak is very close to the surface at depth of  $\leq 0.1$   $\mu\text{m}$ . In addition to the near-surface D peak, SIMS depth profiles from Tiles 7 and 8 typically show also peaks in the intensity of the D signal at the W–Mo and Mo–W interfaces.

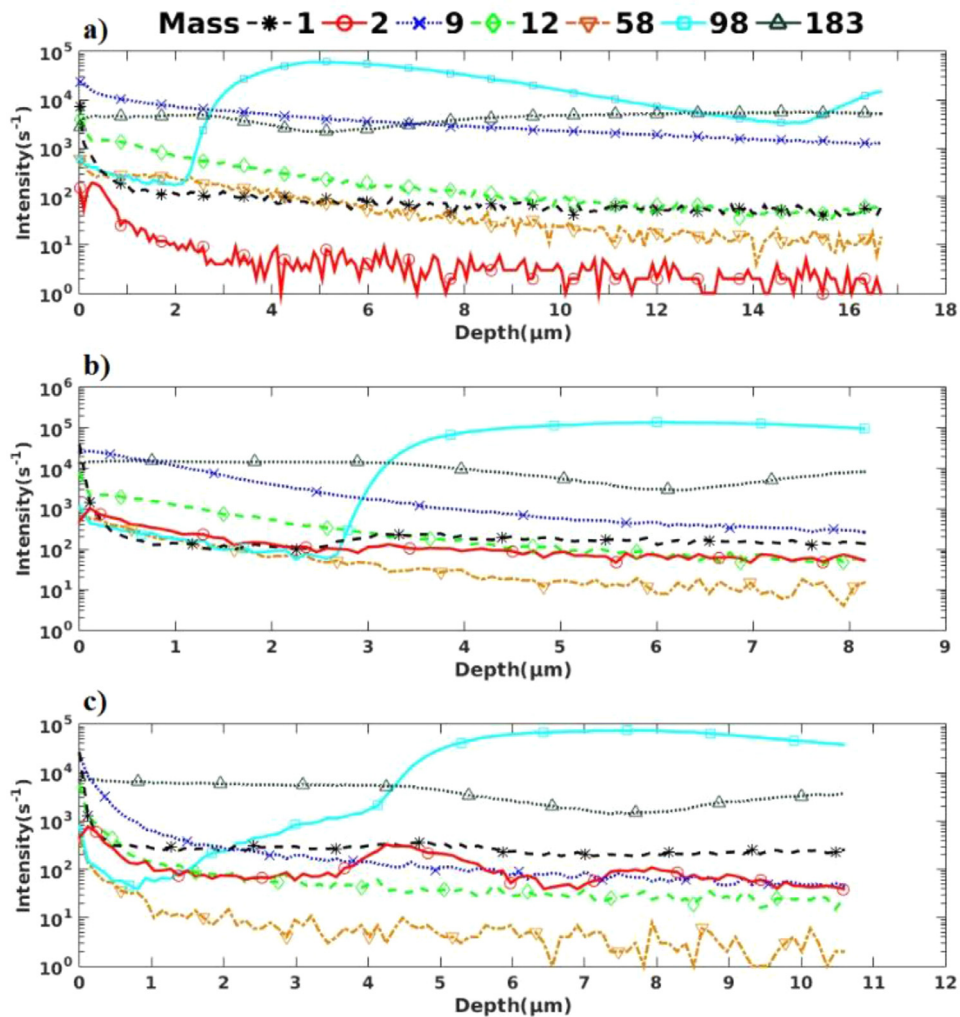


Fig. 4. SIMS depth profiles from a) Tile 6 (2013–2014) ( $S = 1475$  mm), b) Tile 7 (2011–2014) ( $S = 1765.5$  mm) and c) Tile 8 (2011–2014) ( $S = 1877$  mm).

The intensities of these interface peaks are the highest in the lower part of Tile 8. The D retention in the W–Mo and Mo–W interfaces was also observed after the ILW-1 and was found to be dominant retention mechanism in the outer divertor tiles [12].

### 3.3. D retention estimation

The deuterium concentrations ( $\text{at./cm}^3$ ) were determined from the SIMS depth profiles with the help of D-implanted Be, Mo and W samples. The D amounts ( $\text{at./cm}^2$ ) in the SIMS profiles were then integrated from the D concentrations. For the samples from the lower part of Tile 0 and upper part of Tile 1, some of the SIMS measurements were continued until the CFC substrate. The results for these measurement points are integrated from the surface to that depth where the intensity of the C signal starts to increase. However, the intensity of the D signal stays high in the CFC substrate. Since there was no D-implanted CFC sample available, D amounts in the CFC substrate were not included in the quantification and therefore the actual values for those measurement points are thus higher than what is presented here. It is notable that the intensity of the D signal decreases quickly to the background level only in some measurement points from the shadowed part of Tile 4 and the strike point regions on Tile 4 and Tile 6. Elsewhere D have migrated deeper to the samples, intensity of the D signal stays relatively high even deep in the material and measurements could have been continued even deeper.

The D amounts ( $\text{at./cm}^2$ ) for the ILW-2 divertor tiles are shown in Fig. 5 with results for the ILW-1 campaign [3, 4]. The ILW-2 results for most of the measurement points are calculated as an average of more than one measurement. The results for the ILW-2 tiles are generally higher than the data obtained after ILW-1, especially for the lower part of Tile 1, Tile 3, the inner and outer ends of floor Tile 6 and the lower part of Tile 8. The retention profile of D for ILW-2 is quite similar to ILW-1 in the inner divertor. Whereas in the outer divertor, the profile is quite different for Tile 6.

In Tile 0, the D amount is low in the upper part of the tile ( $S < 50$  mm), where the deposits are thin, and higher, up to  $\sim 6 \cdot 10^{18}$   $\text{at./cm}^2$ , in the lower part of the tile ( $S > 50$  mm) where the thickest deposits were formed. In Tile 1, the highest D amounts, over  $8 \cdot 10^{18}$   $\text{at./cm}^2$ , and the thickest deposits are in the upper part of the tile ( $S = 160$ – $270$  mm). In the lower part of Tile 1, D amounts are  $\sim 4 \cdot 10^{18}$   $\text{at./cm}^2$ . Similar to ILW-1 results, the D amounts are higher at both ends of Tile 3 than in the inner strike point region at the central part of the tile, but measured D amounts are higher after ILW-2. In Tile 4, the lowest D amount  $\sim 0.5 \cdot 10^{18}$   $\text{at./cm}^2$  was measured from the inner strike point region around the s-coordinate 800 mm and the highest amount  $\sim 4.5 \cdot 10^{18}$   $\text{at./cm}^2$ , which is higher than for the ILW-1 results for Tile 4, at the inboard side of the inner strike point region. At the outboard side of the inner strike point region, measured D amounts are also higher than for the ILW-1, whereas at both ends of the tile results are close to the ILW-1 results. In the outer diver-

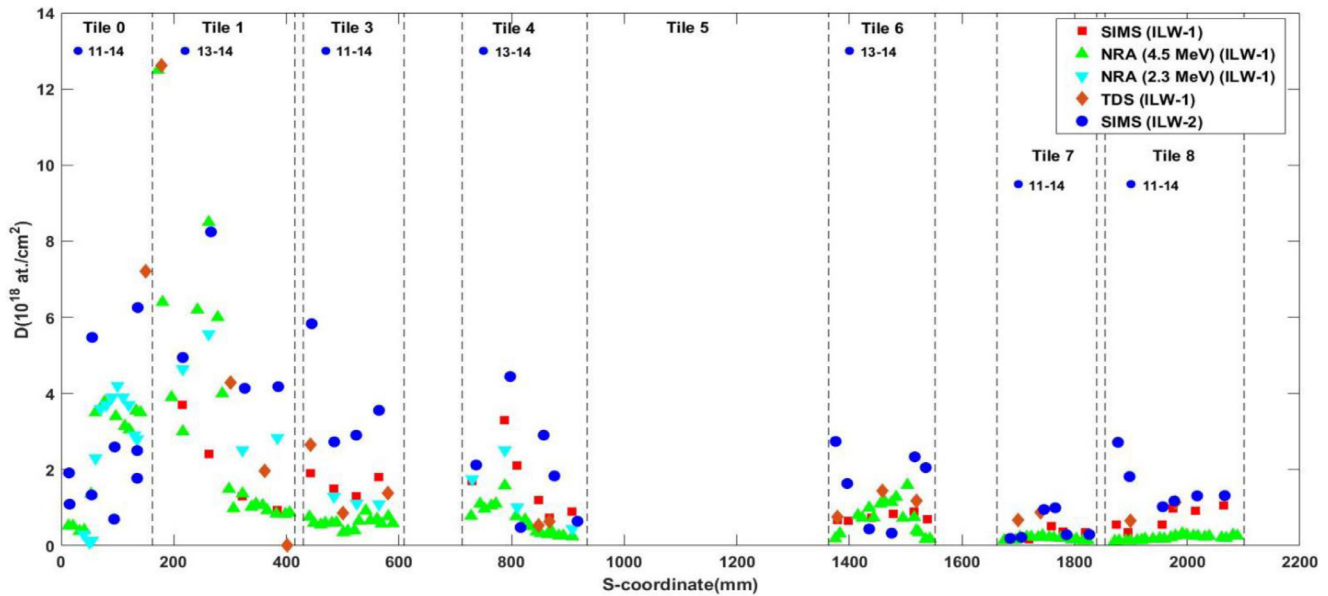


Fig. 5. D amounts ( $\text{at./cm}^2$ ) in the divertor tiles for the ILW-2 and ILW-1 campaigns.

tor Tile 6, the D amount is low  $\sim 0.4 \cdot 10^{18} \text{ at./cm}^2$  in the outer strike point area the center of the tile and higher, up to  $\sim 3 \cdot 10^{18} \text{ at./cm}^2$ , in both sides of the strike point area. In Tile 7, D amounts in the both ends of the tile are similar to ILW-1 measurements, less than  $0.5 \cdot 10^{18} \text{ at./cm}^2$ , but in the center of the tile amounts are higher, up to  $\sim 1 \cdot 10^{18} \text{ at./cm}^2$ . In Tile 8, measured D amounts after ILW-2 are clearly higher than for ILW-1, up to  $\sim 3 \cdot 10^{18} \text{ at./cm}^2$ , in the lower part of the tile where the intensity of the W-Mo interface peaks of D are highest. Whereas in the upper part of Tile 8, D amounts are only a slightly higher than SIMS and TDS results after ILW-1.

The studied Tiles 0, 3, 7 and 8 were exposed during both ILW-1 and ILW-2, and contained already D from ILW-1 campaign, which mostly explains the higher results for these tiles after ILW-2. Increased D retention in the divertor floor tiles 4 and 6 is probably due to the increased ion fluxes to the tiles due to the increased strike point time on these tiles. ILW-2 campaign contained also a larger number of high power plasma discharges. Higher heating power causes more limiter erosion and thus more deposition at the divertor. The higher D amounts measured on ILW-2 samples may also be due to the fact that the SIMS measurements were made deeper than for the ILW-1 samples and as already mentioned, the intensity of the D signal was found to stay relatively high even deep inside the material. After ILW-1, the depth of the SIMS measurements was typically  $< 10 \mu\text{m}$ . Whereas after ILW-2, the measurement depth was more than  $10 \mu\text{m}$  for most of the measurements and the longest measurements reached depths beyond  $60 \mu\text{m}$ . In addition to SIMS measurements, TDS measurements of ILW-1 and ILW-2 samples have also indicated that the D retention is higher for ILW-2 campaign [13].

Samples from both ILW-1 and ILW-2 campaigns were also analyzed by Nuclear Reaction Analysis (NRA), exploring a surface layer of typical thickness  $< 10 \mu\text{m}$ . The good agreement of retained D with different methods for the ILW-1 samples indicates that D has mainly been close to the surface after ILW-1. SIMS measurements after the ILW-2 show in-deep migrated D and ion beam measurements might underestimate the D retention in some parts of the ILW-2 tiles. Tiles 1, 4 and 6 have also been studied after ILW-2 with NRA using 2.3 MeV  $^3\text{He}$  ions [14], which probe the few top-most microns of the surface. The NRA-results are lower than the

SIMS-results, except in the areas where D was observed to be very close to the surface: the strike point regions in Tiles 4 and 6 and the shadowed part of Tile 4.

Plasma isotopic changeover experiments in JET-ILW have shown that hydrogen plasma can reduce retained D mainly from the implanted areas with a very weak access to the codeposited layers [15]. In the deposits of Tiles 0, 1, 4 and 6, the D peak was observed in the depth of  $0.2\text{--}2 \mu\text{m}$  and the depletion of D at the surface is mainly due to the formation of deposits with H on top of the deposits with D during the H plasma phase at the end of ILW-2. Whereas in the low deposition/erosion areas, the depth of the D peak is less than  $0.2 \mu\text{m}$  and the depletion of D at the surface is probably partly due to the isotopic exchange effects.

Deposition on the tiles is non-uniform and it was shown after the ILW-1 using  $\mu\text{-IBA}$  methods that D retention concentrated preferentially on cracks, pits and depressed areas on the surface and more than 70% of trapped D was found in less than 30% of the surface area [16]. To consider non-uniform deposition, more than one SIMS measurement were taken for most of the samples and the results were calculated as an average of the measurements. Some variations were seen between the measurements from the same sample and non-uniform deposition is one possible error source when locally measured values are extrapolated to cover the full divertor surface area.

#### 4. Conclusions

The deuterium amounts ( $\text{at./cm}^2$ ) were determined from the selected ILW-2 divertor tiles removed during the 2014 shutdown using SIMS. Similar to ILW-1, the areas of the highest Be deposition in the inner divertor were found from the lower part of Tile 0 and the upper part of Tile 1. The highest deuterium amounts were  $\sim 8 \cdot 10^{18} \text{ at./cm}^2$  in the upper part of Tile 1, which was exposed only during ILW-2. Be dominated deposition layers were the thickest, up to  $\sim 40 \mu\text{m}$ , in Tile 0, which was exposed during both ILW-1 and ILW-2 campaigns. The thickness of the Be deposition layer in inner divertor Tiles 3 and 4 was  $0\text{--}3 \mu\text{m}$  and in the outer divertor tiles principally thinner than  $1 \mu\text{m}$ , except in the outer divertor floor Tile 6 where deposits with thicknesses  $> 10 \mu\text{m}$  were found  $\sim 30 \text{ mm}$  outward from the predominant outer strike point

position. H peak due to the H plasma phase at the end of ILW-2 was seen at the surface and the D peak was observed deeper. The depth of the D peak was 1.5–2  $\mu\text{m}$  in the thick deposits of Tile 0 and 0.2–0.5  $\mu\text{m}$  in the deposits of Tiles 1, 3 and 6. In the low deposition areas the depth of the D peak was  $\leq 0.2\mu\text{m}$  and the depletion of D at the surface is likely partly due to isotopic exchange during the H plasma experiments at the end of ILW-2.

Deuterium was found to be retained especially in the near-surface layer, thick Be deposition layers and W–Mo interfaces. Measurements show that D have migrated deep into samples and the intensity of the D signal stayed relatively high also deeper in the material, except in the shadowed and the inner strike point areas of Tile 4 and in the outer strike point area of Tile 6, where intensity of the D signal decreases rapidly. Migration of D is probably assisted by the porosity and imperfections due to the original CFC substrate. This porosity-assisted in-deep migration and the interface trapping will probably not be a problem in ITER where bulk W tiles will be used in the divertor.

Measured D amounts in the divertor tiles were generally higher than the results for the ILW-1 campaign. Possible reasons for the higher results are that studied Tiles 0, 3, 7 and 8 were exposed during both ILW-1 and ILW-2 and therefore had  $\sim 2$  times longer exposure time, SIMS measurements of the ILW-2 samples were done deeper compared to the ILW1-samples and changes in the strike point distribution and the plasma conditions between ILW-2 and ILW-1. The downward movement of the inner strike point from Tile 3 to Tile 4 increased ion fluxes to Tile 4 and the change of the outer strike point position from Tile 5 to Tile 6 increased ion fluxes to Tile 6. Moreover, higher heating power in the ILW-2 caused more limiter erosion and thus more deposition at the divertor.

## Acknowledgments

This work has been carried out within the framework of the EUROfusion Consortium and has received funding from the [Euratom research and training program 2014–2018](#) under grant agreement No [633053](#). The views and opinions expressed herein do not necessarily reflect those of the European Commission.

## References

- [1] G.F. Matthews, et al., Phys. Scr. T128 (2007) 137–143. <http://dx.doi.org/10.1088/0031-8949/2007/T128/027>.
- [2] S. Brezinsek, et al., Nucl. Fusion 53 (2013) 083023. <http://dx.doi.org/10.1088/0029-5515/53/8/083023>.
- [3] K. Heinola, et al., Phys. Scr. T167 (2016) 014075. <http://dx.doi.org/10.1088/0031-8949/T167/1/014075>.
- [4] M. Mayer, et al., Phys. Scr. T167 (2016) 014051. <http://dx.doi.org/10.1088/0031-8949/T167/1/014051>.
- [5] E. Joffrin, et al., Nucl. Fusion 54 (2014) 013011. <http://dx.doi.org/10.1088/0029-5515/54/1/013011>.
- [6] F. Romanelli and on behalf of JET Contributors, Nucl. Fusion 55, 2015, 104001. <http://dx.doi.org/10.1088/0029-5515/55/10/104001>.
- [7] C. Ruset, et al., Phys. Scr. T167 (2016) 014049. <http://dx.doi.org/10.1088/0031-8949/T167/1/014049>.
- [8] A. Widdowson et al., Nucl. Mater. Energy (2017) <http://doi.org/10.1016/j.nme.2016.12.008>.
- [9] A. Widdowson, et al., Phys. Scr. T138 (2009) 014005. <http://dx.doi.org/10.1088/0031-8949/2009/T138/014005>.
- [10] J. Beal, et al., Phys. Scr. T167 (2016) 014052. <http://dx.doi.org/10.1088/0031-8949/T167/014052>.
- [11] K. Sugiyama, et al., Nucl. Mater. Energy 6 (2016) 1–9. <http://dx.doi.org/10.1016/j.nme.2015.08.001>.
- [12] H. Bergsaker, et al., Phys. Scr. T167 (2016) 014061. <http://dx.doi.org/10.1088/0031-8949/T167/1/014061>.
- [13] J. Likonen (2016) Unpublished data.
- [14] N. Catarino et al., Nucl. Mater. Energy (2016) <http://dx.doi.org/10.1016/j.nme.2016.10.027>.
- [15] T. Loarer, et al., Nucl. Fusion 55 (2015) 043021. <http://dx.doi.org/10.1088/0029-5515/55/4/043021>.
- [16] H. Bergsaker, et al., J. Nucl. Mater. 463 (2015) 956–960. <http://dx.doi.org/10.1016/j.jnucmat.2014.12.015>.